
Identifying Hand Gestures through Myographic Signals via ANN

Eduardo Coronado
Duke University

Sebastian Knigge
Duke University

Sam Voisin
Duke University

Yuan Zheng
Duke University

Abstract

Lorem ipsum dolor sit amet, consectetur adipiscing elit. Etiam lobortis facilisis sem. Nullam nec mi et neque pharetra sollicitudin. Praesent imperdiet mi nec ante. Donec ullamcorper, felis non sodales commodo, lectus velit ultrices augue, a dignissim nibh lectus placerat pede. Vivamus nunc nunc, molestie ut, ultricies vel, semper in, velit. Ut porttitor. Praesent in sapien. Lorem ipsum dolor sit amet, consectetur adipiscing elit. Duis fringilla tristique neque. Sed interdum libero ut metus. Pellentesque placerat. Nam rutrum augue a leo. Morbi sed elit sit amet ante lobortis sollicitudin. Praesent blandit blandit mauris. Praesent lectus tellus, aliquet aliquam, luctus a, egestas a, turpis. Mauris lacinia lorem sit amet ipsum. Nunc quis urna dictum turpis accumsan semper.

1 Introduction

Recent advances in surface electromyographic signal (sEMG) recordings systems and analytics methods have encouraged the use of sEMGs in human-machine interfaces to control exoskeletons and prostheses; however, challenges remain.¹ Accurate classification of user movements is highly variable given the inherent noise of sEMG recording systems and per-user variability. In turn, this leads to problems downstream when attempting to convert these classifications into spatial directions (e.g. up, down, right, and left). Here, we aim to address the former challenge specifically. Our goal is to design and implement a light-weight unsupervised learning model via a multi-layered neural network to accurately identify six distinct hand gestures from sEMG data.

2 Methods

2.1 Workflow Overview

For this project our workflow was comprised of 4 main phases: preprocessing, dimension reduction via PCA, modeling, and performance comparison as shown in Figure 1 below.

2.2 sEMG Data

Raw sEMG signal data from 36 individuals was obtained online from Lobov et al ². Two series were recorded per individual, each comprised of signals obtained via 8 equally spaced sensors around the forearm (i.e. channels). For each series, subjects were asked to performed a set of 6 basic hand

¹Sergey Lobov & Makarov (2018)

²Ibid

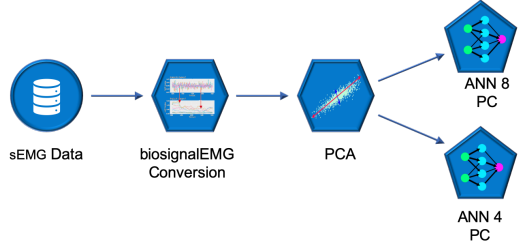


Figure 1: Schematic of overall workflow stages: preprocessing, PCA, modeling and performance comparison

gestures. Each gesture was performed for 3 seconds with a 3 second pause in between. Gestures classification scheme is shown in Table 1.

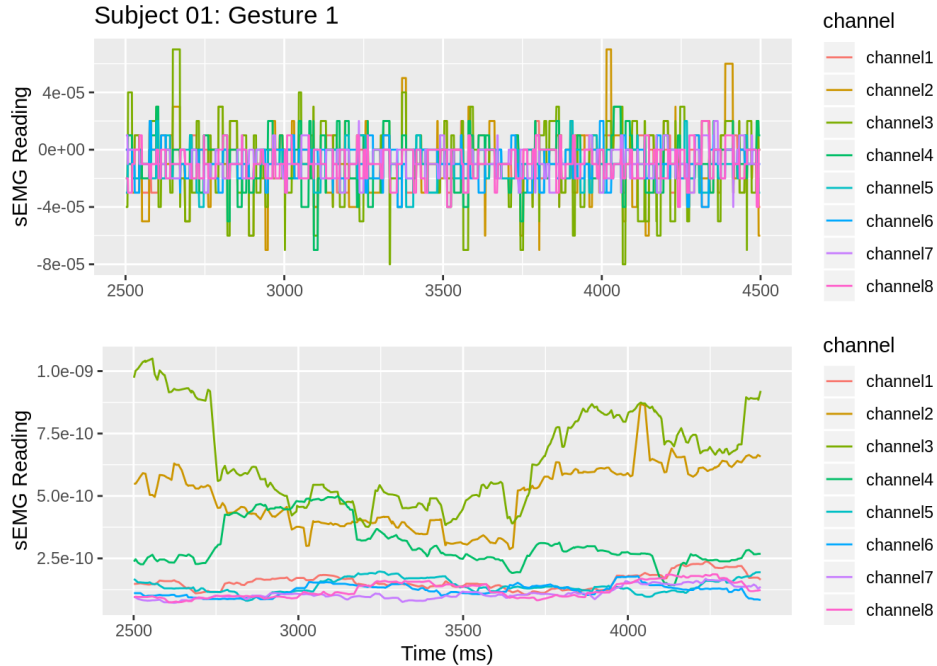
Table 1. sEMG gesture classifications

| Gesture | 1 | 2 | 3 | 4 | 5 | 6 | 7 |
|---------|--------------|-------------------------|---------------|-----------------|-------------------|------------------|---------------|
| | Hand at rest | Hand clenched in a fist | Wrist flexion | Wrist extension | Radial deviations | Ulnar deviations | Extended palm |

2.3 Preprocessing

We implemented a root means squared (RMS) envelope of 200 ms overlapping time windows at 100ms steps via the *biosignalEMG* R package³ to remove some of the noise generated during sEMG signal collection. As shown in Figure 3 the pre-processing does help provide a means to generate clearer signals that show distinct patterns from each channel per gesture

Figure 3: Schematic of overall workflow stages: preprocessing, PCA, modeling and performance comparison



Subsequently, the data was separated according to the gesture classifications (1-6) provided for each time step for further analysis.

³J.A. Guerrero (2018)

2.4 Dimension Reduction

Dimension reduction for each gesture was done via a principal component analysis (PCA) of the 8 distinct channels used to record sEMG data in order to identify the most relevant channels for gesture classification and potentially reduce the training time of the neuronal network. We achieved this via the R *princomp* function that performs a spectral decomposition via singular value decomposition (1) of the gesture design matrix (\mathbf{X})

$$\mathbf{X} = \mathbf{U}\mathbf{D}\mathbf{V}' \quad (1)$$

where \mathbf{U} and \mathbf{V} are the row and column space eigen vectors and \mathbf{D} is a diagonal matrix with the eigen values.

2.5 Modeling

Before fitting an Artificial Neural Network (ANN) we "padded" the ends of each gesture's data matrix to ensure that the vectors passed into the models are of equal dimension. We then developed two ANN with one hidden layer, the first with all components and a second with channels subset selected during the dimension reduction stage (Figures 4a and 4b, respectively). Each of these has a single hidden layer with eight hidden nodes having linear activation. These eight nodes feed into six output nodes with a soft-max activation function. This model was inspired by Lobov et al's approach.⁴

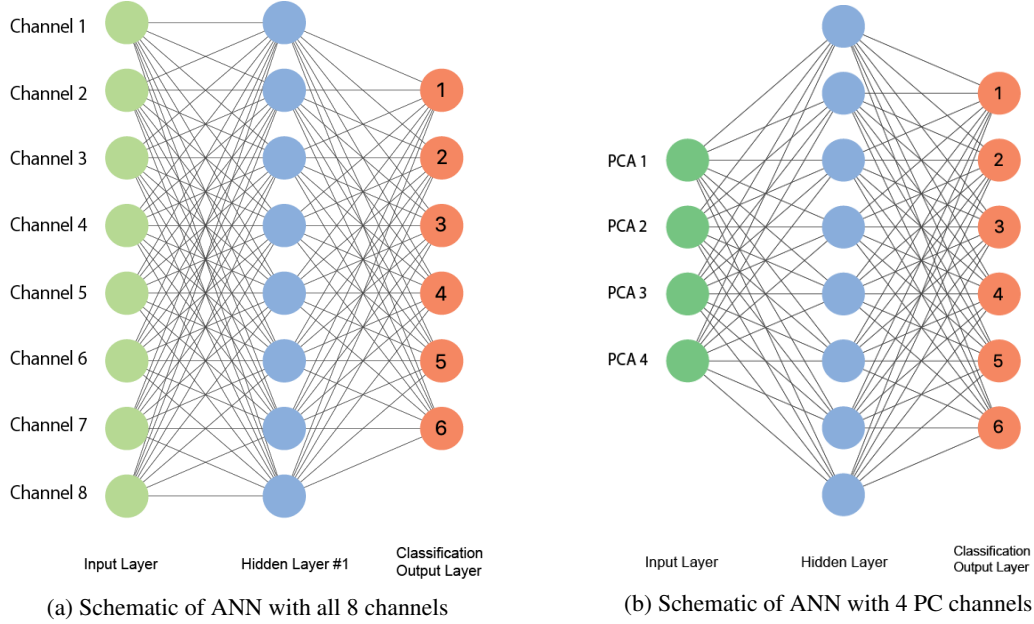


Figure 4: Artificial Neuronal Net structures

The computation graphs for the ANN were generated via an R implementation of Keras⁵, which relies on Google's TensorFlow engine for backpropagation. This allowed us to implement a flexible design framework so that we could add, edit, and remove layers from our models quickly and efficiently during our development process.

Afterward, five additional ANN were generated with an increasing number of hidden layers ($l = 1, \dots, 5$) but only using the principal components as inputs. Figure 5 shows a schematic representation of how each hidden layer was added following a similar process for inputs and outputs as for the initial ANNs.

2.6 Performance Assessment

To assess the performance of each ANN, we used an k-fold cross validation strategy ($k = 5$) to split our data to generate a gesture-specific training and a testing sets. These were using the *caret*

⁴Sergey Lobov & Makarov (2018)

⁵Daniel Falbel (2019)

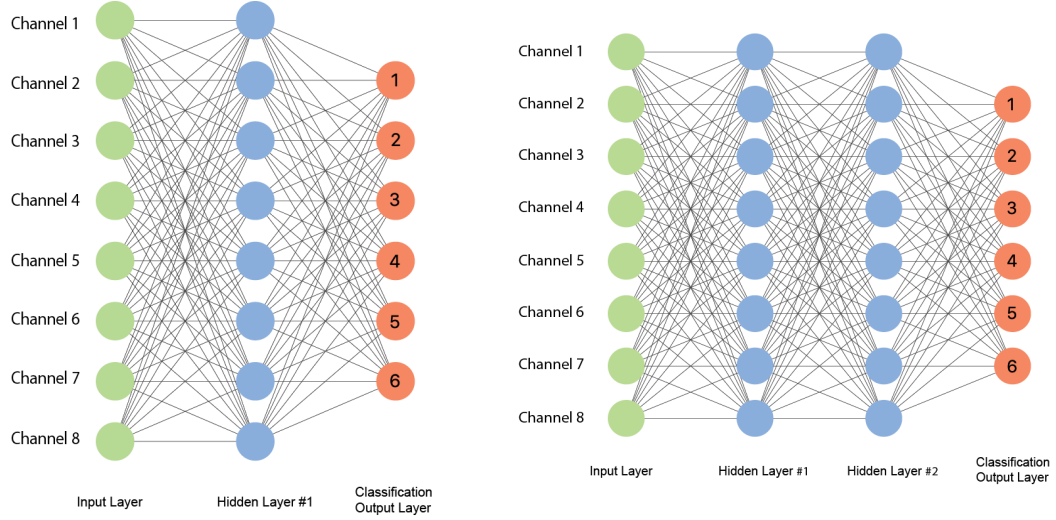


Figure 5: Increasing number of hidden layers in Artificial Neuronal Net structure

R package via random sampling. We then assessed the average classification accuracy of each ANN using a categorical cross entropy metric which measures the *Kullback-Leibler* (KL) divergence between the true distribution of the response variable and the distribution of the predictions. This was done for both the initial ANN previously mentioned and shown in Figures 4a and 4b, as well the subsequent ANN with increasing number of layers from Figure 5.

Additionally, our code was timed to assess the computational costs versus gains in accuracy as we increase the number of layers.

3 Results

3.1 Principal Component Analysis

Using the spectral decomposition we found that only 4 of the 8 principal components in our dataset contributed meaningfully to variance in our response. From figure 3, we can see that these 4 components account for approximately 80% of the variability we are seeking to model.

We might be interested in comparable results, or a decision rule which is applicable to different data sets. We introduce a relative measure κ which can be used for the PCA of data sets with any dimension.

$$\kappa_i = \frac{\text{proportional explained variance}_i}{\frac{1}{\# \text{ of dimensions}}}$$

One can define a decision rule, which is dependent on a threshold δ : *Include* $PC_i \forall \kappa_i > \delta$

For our data set we choose $\delta := 0.6$.

Figure 6: PCA Screeplot and cumulative variance plot

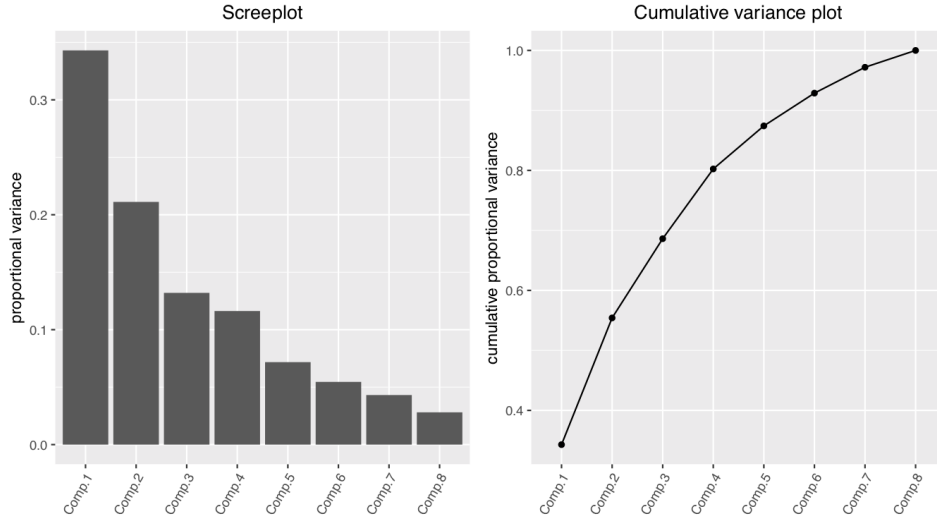


Table 1: PCA measures

| | Comp. 1 | Comp. 2 | Comp. 3 | Comp. 4 | Comp. 5 | Comp. 6 | Comp. 7 | Comp. 8 |
|----------------------------------|---------|---------|---------|---------|---------|---------|---------|---------|
| proportion of explained variance | 0.343 | 0.211 | 0.132 | 0.116 | 0.072 | 0.055 | 0.043 | 0.028 |
| cummulative explained variance | 0.343 | 0.554 | 0.686 | 0.802 | 0.874 | 0.929 | 0.972 | 1 |
| κ | 2.744 | 1.689 | 1.056 | 0.930 | 0.574 | 0.437 | 0.345 | 0.225 |

By reducing the number of inputs from 8 smoothed signals to only 4 principle components, we were able to reduce overfitting in our model prior to ultizing any dropout layers. This reduction in overfitting decreased prediction accuracy in the validation data set only slightly see the *ANN Performance Comparison* section.

3.2 ANN Performance Comparison

From the timing table for every number of layers (layer), we can see that the most time-wasting method is 4 layers ANN, which will take about 556s on the test dataset, while the fastest method is 1 layer ANN, which will take about 300s on the same dataset. It turns out that 5 layers ANN is less time wasting than 4 layers ANN, which only takes about 500s. Considering the remarkable improvement on the performance after using the multiple layers ANN, the little amount of time sacrifice on the computation is totally acceptable.

References

- Daniel Falbel, e. a. (2019). Package ‘keras’ [Computer software manual].
- J.A. Guerrero, J. M.-D. (2018). Package ‘biosignalemg’ [Computer software manual].
- Sergey Lobov, I. K. V. K., Nadia Krilova, & Makarov, V. A. (2018). Latent factors limiting the performance of semg-interfaces. *Sensors*, 18(1122).